Statistical Investigations of Parameters that Drive High-Shear Granulation

by

Michael Loren Lay

A Thesis Presented in Partial Fulfillment
of the Requirements for the Degree
Master of Science

Approved April 2019 by the
Graduate Supervisory Committee:

Heather Emady, Chair
Christopher Muhich
Julianne Holloway

ARIZONA STATE UNIVERSITY

May 2019

ABSTRACT

Granulation is a process within particle technology where a liquid binding agent is added to a powder bed to create larger granules to modify bulk properties for easier processing. Three sets of experiments were conducted to screen for which factors had the greatest effect on granule formation, size distribution, and morphological properties when wet granulating microcrystalline cellulose and water. Previous experiments had identified the different growth regimes within wet granulation, as well as the granule formation mechanisms in single-drop granulation experiments, but little research has been conducted to determine how results extracted from single drop experiments could be used to better understand the first principles that drive high shear granulation. The experiment found that under a liquid solid ratio of 110%, the granule growth rate was linear as opposed to the induction growth regime experienced at higher liquid solid ratios. L/S ratios less than 100% led to a bimodal distribution comprised of large distributions of ungranulated powder and large irregular granules. Insufficient water hampered the growth of granules due to lack of enough water bridges to connect the granules and powder, while the large molecules continued to agglomerate with particles as they rotated around the mixer. The nozzle end was augmented so that drop size as well as drop height could be adjusted and compared to single-drop granulation experiments in proceeding investigations. As individual factors, neither augmentation had significant contributions to granule size, but preliminary screens identified that interaction between increasing L/S ratio and decreasing drop size could lead to narrower distributions of particles as well as greater circularity. Preliminary screening also identified that decreasing the drop height of the nozzle could increase the rate of

particle growth during the 110% L/S trials without changing the growth mechanisms, indicating a way to alter the rate of steady-state particle growth. This paper screens for which factors are most pertinent to associating single-drop and wet granulation in order to develop granulation models that can ascertain information from single-drop granulations and predict the shape and size distribution of any wet granulation, without the need to run costly wet granulation experiments.

ACKNOWLEDGMENTS

I would like first off to thank my parents who have supported me through my 18 years of academia, always encouraging me to focus on my vocation as a student and worry about work later.

I would like to thank the NASA Space Grant program for funding the first year of my Thesis.

I would like to thank Dr. Emady for giving me the opportunity to research with her the past four years, and has always been understanding of my roadblocks and encouraging of scholastic pursuit. I would like to thank her two Ph.D students, Manogna Adepu and Tianxiang Gao who critiqued my work and showed me the process of high-level academic writing. I would like to thank Nicole Martin who helped me conduct experiments and analyze results. And lastly I would like to thank Brandon Boepple, my co-graduate in the 4+1 program whose keen eye and thoroughness kept me accountable during the last two years of the Master's.

TABLE OF CONTENTS

LIST OF TABLES

Table Page

Table Page

LIST OF FIGURES

Figure Page

Figure Page

LIST OF SYMBOLS

Symbol Page

CHAPTER 1

INTRODUCTION

Particle processing is a field within chemical engineering that focuses on the formation, characterization, and transport of solid particles. Unlike fluids, the theoretical behavior of solids cannot be predicted solely from state properties. In the United States alone, particle-based products contribute more than 1 trillion dollars to the national economy and encompass products from crystals to pastes to granules (Litster, 2016). Paramount to the pharmaceutical, food, agricultural, and myriad other commercial uses, particles and consequently the mechanisms by which they are produced and characterized, create a specialized field that can be studied using traditional chemical engineering methodologies, but with significantly different relations than traditional fluid mechanisms. The flow behavior of most fluids can be accurately modeled with a few thermodynamic properties defined. The rheological properties of solids, and specifically particles, however, are also contingent on the size distribution, shape, densities, solidity, internal structure, roughness, and strength inherent to a set of particles. The understanding of how the aforementioned particulate properties and apparatus configurations affect final particle products leads to innovation and optimization at all stages of particle processing. This paper focuses on screening for the key parameters that affect the morphological and size properties of a batch of granules, and how the parameter trends can be related to single-drop parameters to use in future quantitative models of granulation.

CHAPTER 2

BACKGROUND

Granulation is the process of adding a liquid binding agent to a bed of small particles to create larger granules (Litster, 2016). Two common forms of granulation are single drop and high-shear granulation, that focus on the formation of single granules and large distributions, respectively. Single drop granulation focuses on quantifying the effect one drop will have on a static bed, and literature has shown that the three primary mechanisms in which a single drop can form a granule in a single bed are tunneling, spreading, and cratering (Emady, Kayrak-Talay, Schwerin, & Litster, 2011). Emady *et al*. have quantified that the drop impact velocity as well as powder properties are the key mechanisms that dictate the rate and shape of the final granules formed, and that ideally a low drop velocity and powder bed that exhibit tunneling behavior will create round granules, the most practical granule shape for industrial use. Other studies have shown that the effects of nozzle size and drop frequency can be calculated to predict the size of a single granule formed from a single drop (Wildeboer, Koppendraaier, Litster, Howes, & Meesters, 2007). From single drop granulation experiments, scientists can glean information about particle, liquid, and apparatus relationships that can be used to design improved wet granulation processes.

The three primary forms of batch granulation are fluidized granulators, tumbler granulators, and mixer or high-shear granulators. Central to the understanding of both single-drop and batch granulation is the success of nucleation, or the process in which fine powders coalescence to create the nuclei of that granule (Litster, 2016). An understanding

of nucleation has allowed for the development of a regime map which characterizes the three primary forms of nucleation: drop controlled, where a single drop creates a single granule and yields the most narrow particle distribution; mechanical dispersion, where the size distribution of granules depends predominantly on liquid-particle interactions and the mechanical shear of the granulator; and a middle intermediate regime, where particles are neither mechanical nor drop dominated, but are greatly influenced by even small variations in granulator operating conditions. Hapgood *et al*. developed a regime map that plots a dimensionless spray flux, Ψa, which relates the liquid volumetric flow rate, drop size powder surface velocity, and the width of the spray zone, versus the drop penetration time as calculated by the Washburn method (Hapgood, Litster, & Smith, 2003; Heertjes & Kossen, 1967). A figure of the regime map can be seen below in Figure 1.

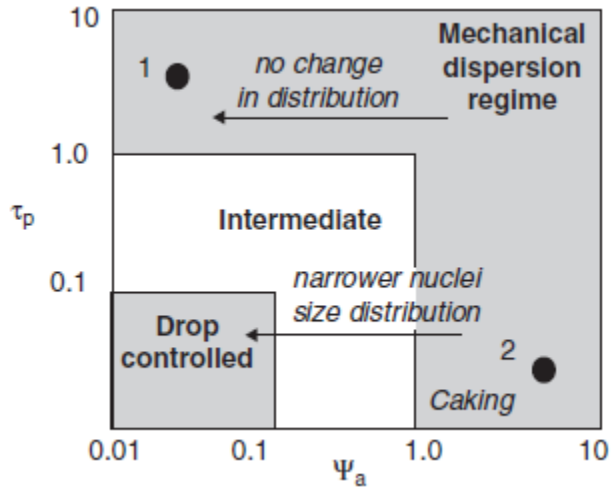

Figure 1. A regime map for wet granulation, plotting penetration time, τ_p, versus dimensionless spray flux, Ψa, from Design and Processing of Particulate Products (Litster, 2016)

The regime map is a key resource in deciphering the parameters that affect granulation, but is limited in that the regimes give a starting point of how to narrow the particle

polydispersity without quantifying specific distributions or other important characteristics of produced granules. Badawy *et al.* have demonstrated the inversely proportional relationship between starting primary particle size and rate of granule formation (Badawy & Hussain, 2004). Another correlation that quantifies the behavior of granulation growth and consolidation over time is the Stoke's number, which compares the effects of particle density, yield strength and collision velocity to determine the dynamic strength, or essentially malleability, of granules as they grow in size (Bouwman *et al.*, 2005). The Stoke's deformation number is used to predict whether or not a particle will experience steady-state growth, characterized by large deformations of granules upon collision, leading to consistent coalescence, or induction growth, where particles deform little upon collision, and instead granules grow in size primarily through layering. These two effects have been visualized in the Figure 2., which highlights how growth rate of particles can be affected by moisture content, instead of other parameters that may increase growth rate.

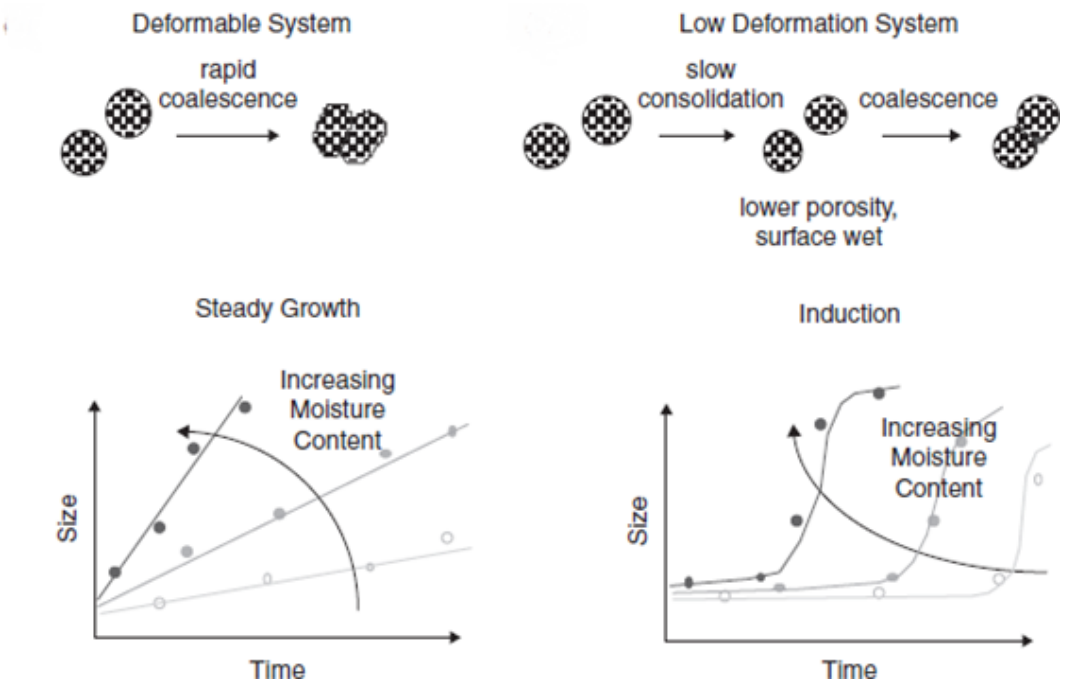

Figure 2. An image of the two main growth mechanisms in wet granulation, steady growth and induction, adapted from Design and Processing of Particulate Products (Litster, 2016).

Scott *et al*. have found that melting the binding agent in situ with the powder can hinder the overall size and rate at which particles develop, without sacrificing the heterogeneity of the final particle distribution (Scott, Hounslow, & Instone, 2000). Models, such as the coalescence model, purport methods to calculate particle size distribution, size, and morphology, based on first principles, and have made large steps in replacing large expensive experiments with computer modeling (Pohlman & Litster, 2015). Currently, models are insufficient to completely predict the pertinent properties of particles post processing, but further understanding of correlations between single-drop and batch granulation make computer modeling more robust, and pilot scales smaller and cheaper to execute.

The current literature on granulation mechanisms have identified which granulation variables affect granulation rates and granule properties. However, in order to create more precise granulation models, specific quantitative relationships between parameters and granule size and shape must be developed. This project focuses on identifying the effects most significantly affect granule formation, and correlating the findings from single-drop and wet granulation experiments so future work can further the progress of quantitative granulation models.

CHAPTER 3

METHODS

3.1 Procedure

Each set of experiments was a screening DOE of at least 8 trials and at least one replicate per trial. A mass of 150 or 250 grams of fine microcrystalline cellulose (MCC) was measured and placed in a 5-liter KG5 high shear granulator/mixer seen below in Figure 3.1.

Figure 3. The container and impellor (left) for the KG5 High Shear Granulator (right).

Before each trial, the volumetric spray rate was calibrated by measuring the volume of water collected in a graduated cylinder per minute. Each trial consisted of a 5 minute dry mixing stage to ensure there were no clumps in the powder bed prior to the granulation process. The dry mixing was proceeded by the spraying, the time of which was dictated by the product of the L/S ratio and the volumetric spray rate. After the spraying ceased, each trial was allowed to wet-mass for 60 minutes, with 10 g samples of the particles being moved from the batch every 15 minutes, starting at minute 0. When the granulation finished, all the remaining granules were placed in an oven-safe container and dried at 75°C

for 48 hours. After drying, the weight distribution of particle size for each sample in a trial was calculated using sieve analysis.

Figure 4. The electric sieve shaker (left), and example 12" diameter sieves (right) used to separate dried granules by size.

Thirteen sieves with mesh apertures ranging from 180 microns to 2 millimeters were sieved for ten minutes in an electric sieve shaker, as seen in Figure 4 above. Granules larger than 4 mm or dried cake from the granulator were removed so that they did not confound the weight distributions of the particles size (see Figure 5 below).

*Figure 5. Microcrystalline Cellulose (*MCC) and water combinations larger than 4 mm taken from an experiment trial (2/18/19) that consisted of a 120% L/S ratio, high drop height, and large drop size.

In the third experiment, particles that had a diameter between 1.00 and 1.18 mm that were formed from 120% L/S batches were characterized in a Malvern Morphologi G3; an instrument that uses optical spectroscopy to measure particle size, as well as solidity, shape, and myriad other parameters, seen in the Figure 6.

Figure 6. Malvern Morphologi G3, used to identify shape factors for 120% L/S trials in Experiment 3.

Solidity, particle diameter, and circularity were measured and then analyzed in JMP to look for statistically significant differences in particle shape.Solidity measures the concavity of a particle; Circularity quantifies the degree to which a particle is similar to a circle. JMP was also used to calculate how mean particle size and particle variance were affected by the parameters changed in Experiment 3.

3.2 Parameters

This thesis is based on three experiments that used three different statistical designs of experiments to change a combination of liquid-solid (L/S) ratio, granulator impellor speed, volumetric spray rate, liquid drop size, and liquid drop height. The goal was to investigate

the effects each parameter had on size distribution and in some cases morphological properties as well. Each experiment was a screening design used to identify the most prudent factors, so that additional experiments could be used to better quantify the effect a particular parameter had on the final size distribution of the granules.

L/S ratio is a mass ratio between the amounts of binder agent, in this case water, to the mass of the particle bed, microcrystalline cellulose (MCC). The L/S ratio was varied in every experiment, with values ranging from 80% to 130%. The granulator impellor speed was a parameter on the KG5 granulator that affected the shear incurred by the particle bed, and could vary between 75 and 750 rpm, although these experiments avoided high-shears to avoid operating in the mechanical dispersion regime when possible. Volumetric spray rate was usually kept below 20 ml/min, and in the first experiment was also altered to account for different wetting times. Since the KG5 only came with one spray nozzle, drop size was altered by adding a syringe tip to the end of the nozzle, and reducing the volumetric spray rate to ensure the syringe would not fall into the bed. An image of the two syringe tips is seen below in Figure 7.

Figure 7. On the left, the large (2 mm) and small (0.2 mm) syringe nozzles, and on the right, the modified syringe apparatus attached to the spray nozzle.

The drop height could only be altered by approximately 3 cm, and was changed by moving the entire nozzle in the granulator, as seen in Figure 7 above.

3.3 Summary of DOEs

Tables 1, 2, and 3 below show the initial factors and levels for the 8 trials that were run for each experiment.

Table 1. Design of experiment for Experiment 1, varying wetting time, L/S ratio, and impellor speed.

Combination	Wetting Time (min)	L/S Ratio	Impellor Speed (rpm)
1	10	80%	250
2	10	80%	325
3	10	90%	250
4	10	90%	325
5	20	80%	250
6	20	80%	325
7	20	90%	250
8	20	90%	325

Table 2. Design of experiment for Experiment 2, varying drop height and L/S ratios above 100%. 250 grams of MCC were granulated with MCC at a flowrate of 10 ml/min,

Combination	Drop Height	L/S Ratio
1	High	100%
2	High	110%
3	High	120%
4	High	130%
5	Low	100%
6	Low	110%
7	Low	120%
8	Low	130%

Table 3. Design of experiment for Experiment 3, varying L/S ratio, drop height, and drop size.

Combination	L/S Ratio	Drop Height	Drop Size
1	120%	High	Large
2	120%	High	Small
3	120%	Low	Large
4	120%	Low	Small
5	80%	High	Large
6	80%	High	Small
7	80%	Low	Large

8	80%	Low	Small

CHAPTER 4
PRELIMINARY INVESTIGATION OF HIGH-SHEAR GRANULATION

4.1 Introduction

The purpose of the first experiment was two-fold, to screen for parameters that affected granulation, but also to understand the mechanics of the KG5 high shear granulator. This 3-parameter 2-level factorial design of experiment chose impeller speed, L/S ratio, and volumetric spray rates based on similar experiments with zirconium hydroxide and the same granulator (Adepu *et al*., 2016). There were 16 trials that granulated 250 grams of MCC with water ratios of 80% or 90% L/S, wetting times of 10 or 20 minutes, and impellor speeds between 250 and 325 rpm. The results are seen below.

4.2 Results

The parameter that had the most obvious effect on both mean particle size as well as distribution patterns was the L/S ratio. An average cumulative distribution of the mass percentage of particles versus the sieve size was used to quantify the polydispersity of the granules, seen in Figure 8. Error bars were calculated using the standard deviation between trials, but were omitted for graph clarity-they can be found in Appendix B-1.

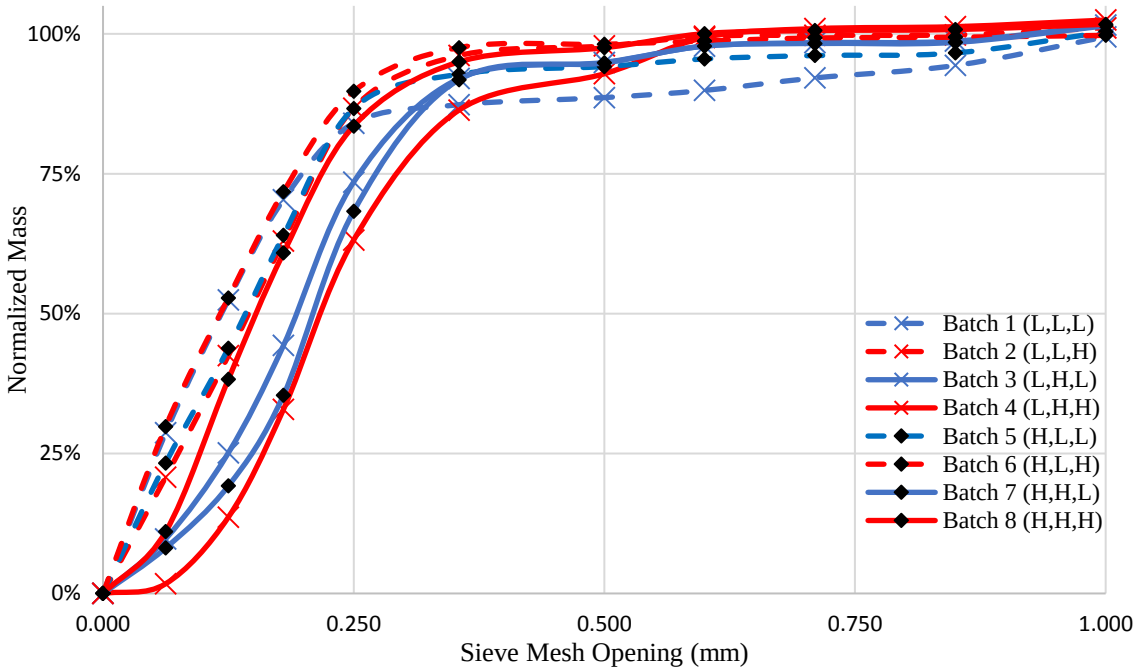

Figure 8. The normalized mass distribution versus the sieve mesh opening for the 8 trials in Experiment 1. The blue line is the lower impellor speeed, the dashed line is the lower L/S ratio, and then 'X's are the decreased wetting time. H and L represent high and low levels for each parameter.

The figure above demonstrates that for each batch, the combination with the higher L/S ratio, solid line, had a higher mean particle size. The batches with the greater L/S ratio had a d_{50} value .07 mm greater than the batches with the lower L/S, except Batch 4 which had a lower wetting time and greater impellor speed. Figure 8 above was used to calculate the d_{10}, d_{50}, and d_{90} for each of the batches, seen below in Table 4.

Table 4. The d_{10}, d_{50}, and d_{90} distributions for the average value of the 8 trials in Experiment 1.

Batch #	d10	d50	d90	d50/d10	d90/d50	d90/d10
1	0.022	0.118	0.606	5.4	5.1	27.5
2	0.030	0.145	0.271	4.8	1.9	9.0
3	0.064	0.193	0.355	3.0	1.8	5.5
4	0.110	0.216	0.408	2.0	1.9	3.7
5	0.026	0.142	0.279	5.5	2.0	10.7
6	0.020	0.117	0.252	5.9	2.2	12.6
7	0.075	0.209	0.340	2.8	1.6	4.5

8	0.057	0.152	0.293	2.7	1.9	5.1

Batches 3,4,7,8 (high L/S ratios) all have smaller d_{50}/d_{10} and d_{90}/d_{50} and higher d_{50} values, representing tighter particle size distributions and larger mean particle size, respectively. The d_{50} values were analyzed in JMP to further identify trends, and while neither wetting time nor impeller speed had significant effects on their own, the combination of either high-high or low-low decreased the d_{50} particle size by .04 mm, while either low-high combination increased the particle size by .03 mm. The four trials run at lower L/S ratios all had d_{10} values lower than .03 mm, and d_{50}/d_{10} values greater than 5, showing both a significant amount of powder remaining after the wet granulation and a wide size distribution of fine particles.

4.3 Discussion

Despite lower L/S ratios being sufficient to effectively granulate zirconium hydroxide in other experiments, an L/S ratio of 80% left large amounts of MCC as un-granulated powder, leading to a wide particle size distribution with large amounts of powder smaller than 80 micron and large d_{50}/d_{10} value (Adepu *et al*., 2016). Studies have shown that an increase in hydrophobicity leads to spreading behavior during the nucleation phase, when the powders begin to form a fine layer across a drop of water liquid as the liquid comes in contact with the bed, which in turn leads to a smaller average granule size due to weaker liquid bridges between MCC particles (Nguyen, Shen, & Hapgood, 2010). Thus, the chemical nature of MCC requires at least a minimum liquid solid ratio greater than 80% to ensure each granulated batch is not left with large amounts of un-granulated powder. Hydrophobicity and wetting are parameters between liquid and solid powder beds in

single-drop granulation experiments, thus if the effect chemical properties on wet mass granules average size and strength, single drop experiments can be used to identify an effective starting L/S ratio for a mean desired granule size.

The wet granulation performed in this experiment does not create individual drops of liquid, but rather an intermittent stream, due to the higher volumetric spray rates of both the short and long wetting times. The fact that wetting time had relatively little effect on mean granule size signifies that both levels had spray fluxes sufficiently high so drops were overlapping and falling out of the drop controlled region in the nucleation regime map seen in Figure 1. However, as the wetting time increased and the impellor speed decreased, or when the wetting time decreased but the impellor speed increased, the average particle size increased, indicating an important cross-relationship between spray rate and shear rate. Since the strength of particles is inversely proportional with size and shear rate, it is likely that the lower impellor speed and a higher wetting time allowed more time for nucleation and less shear to break the particles, while the lower wetting time and higher shear created stronger smaller particles during nucleation that continued to grow during the wet-massing time (Litster, 2016). The effects of spray rate and shear rate achieve different purposes within granulation, thus their combined effects must be further studied to quantify precisely how their combined mechanisms affect the growth rate of granules during extended wet granulation periods.

The high and low level of the impellor speed were too similar for any meaningful individual effect to be quantified, but literature has shown that increasing the impellor speed directly reduces the average size and subsequently increases the average strength of the smaller

granules (Nguyen *et al*., 2010). Since impellor speed is an instrument parameter, a low impellor speed was used for the remaining experiments to better mimic single-drop granulation conditions.

CHAPTER 5

INVESTIGATION OF MOISTURE EFFECTS OVER TIME

5.1 Introduction

As demonstrated in Experiment 1, the L/S ratio had the greatest effect on size distribution; therefore, the second experiment honed in on identifying how L/S ratios from 100% up to 130% would affect the mean particle size. In addition to the effects of hydration, this experiment wanted to screen for the effects of drop heights because the relationship between single-drop and wet granulation was obvious. This experiment ran 8 trials and investigated the effects of the aforementioned parameters on particle size distribution after the entire granulation, as well as how the distribution changed throughout the 60-minute wet-mass time. The results are discussed below.

5.2 Results

Similar to Experiment 1, the L/S ratio had the greatest effect on the particle weight distribution at 60 minutes, as well as throughout the wet massing time. In comparison, the effect of lowering the height of the nozzle had a noticeable, but miniscule effect on the cumulative particle distribution of particles less than 1.18 mm. With the exception of 110% L/S ratio, the lower nozzle height had a greater particle size at d75. For the 100% and 110% L/S ratio, the d25 particle size was about .05 mm smaller for the higher nozzle height. Standard deviation error bars were omitted from these results as well due to the cluttering

nature of having so many error bars stacked at each sieve mesh size.

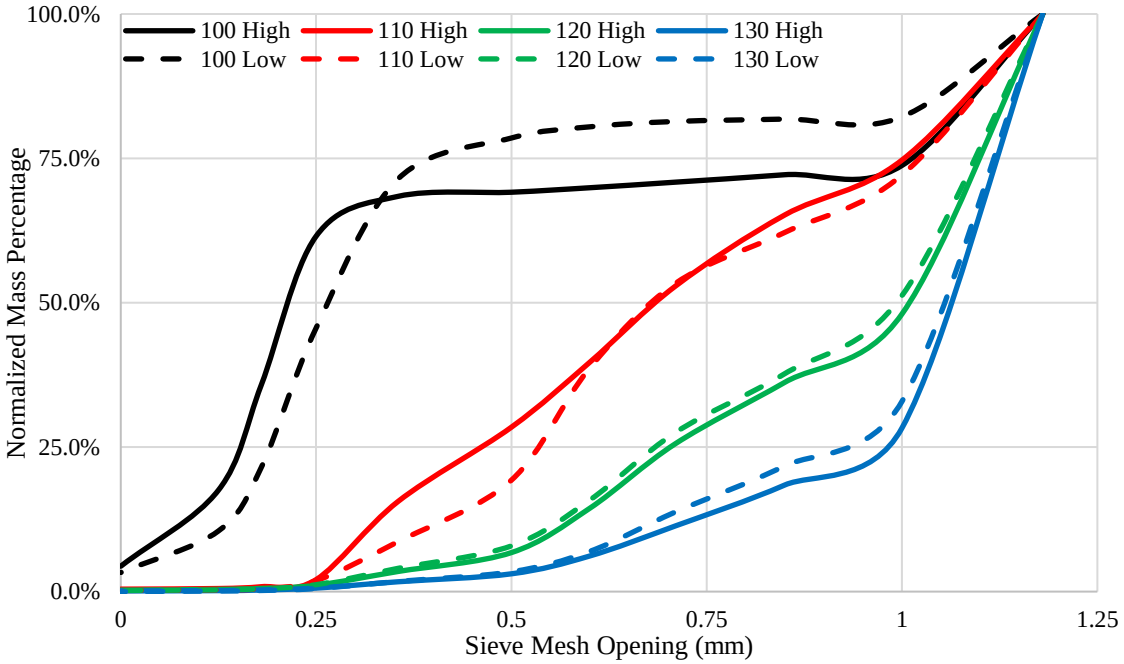

Figure 9. The normalized mass distribution versus the sieve mesh opening for the 8 trials in Experiment 2. The different colors represent different L/S ratios, and the dashed lines represent a low drop height.

Similar to Experiment 1, the 100% L/S ratio demonstrates an "S-Curve" behavior. The three higher L/S ratio curves, however, are still rapidly rising at end of the distribution, indicating the sieve meshes used were insufficient to capture the full size distribution for these higher hydration trials, seen in Figure 9. In order to understand the behavior over time, it was important to calculate a specific size distribution and track its growth over time. For 120% and 130% L/S ratio, the d50 value is larger than 1 mm. Also, for every curve besides 100% L/S low nozzle height, the d75 value is above 1 mm. Therefore, to accurately demonstrate the growth of granules during the 60-minute wet-massing period, the d10 value was sampled and calculated for each trial, as seen in Figure 10 below.

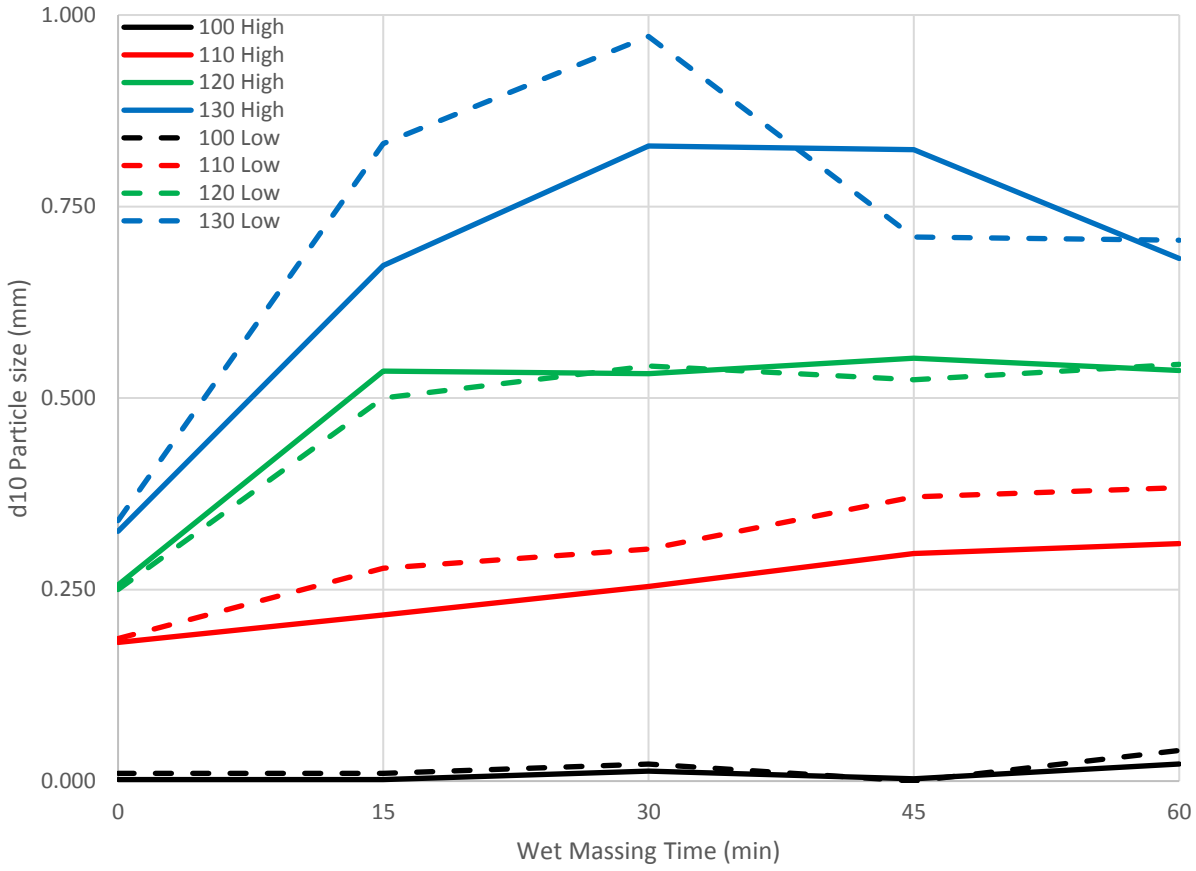

Figure 10. The d10 particle size in mm as a function of wet massing time for the 4 different L/S ratios and different drop heights in Experiment 2.

In Figure 10 above, both the 100% and 110% L/S ratios demonstrate relatively linear growth in d10 particle size over time, albeit the slop of the 110% L/S ratio increases more rapidly. The rate of d_{10} particle growth over for the low drop 110% L/S ratio is larger than its high drop experiment of similar parameters. For 120% L/S ratio, both high and low nozzle heights, the d10 particle size increased rapidly in the first 15 minutes, then was relatively unchanged at just above .500 mm for the remaining 45 minutes of wet-massing. The 130% L/S ratio exhibits a steeper increase in particle size over the first 30 minutes

than the 120% L/S trials, but then the d10 particle size decreases for the remaining 30 minutes. The lower drop height demonstrates both a more dramatic particle growth rate (21 microns per minute) as well as a more severe particle shrink rate (-17 microns per minute), than the higher nozzle drop which growth rates of 16 and -9.4 microns/minute respectively.

5.3 Discussion

While Figure 9 above clearly demonstrated that there was a significant increase in the median particle size as the L/S ratio increased, the lack of sieves with a mesh greater than 1.18 mm hindered discovering the full distribution behavior of the greater hydration trials. However, as the L/S ratio increased, the d10/d50 ratio decreased, demonstrating a complete shift away from having un-granulated powder, and an increase in mean particle size. The results in Figure 10 corroborate the patterns observed in the literature, that increasing the L/S ratio increases the mean particle size, a trend also observed in Experiment 1.

Figure 10 above contrasts the two different growth behaviors for high hydration granules, induction, and steady growth (Iveson & Luster, 1998). For both low and high drop heights, the 110% L/S ratio granules grow under the steady growth/linear regimes. At appropriate hydration ranges, the rate at which particles grow increases with increasing moisture content, but the lower drop height demonstrates that growth rate can also be affected by drop height. The effect of drop height on steady growth rates is an important relationship because it presents another way to control average granule size, without adding so much moisture that the growth regime changes to induction, as seen by the behavior of the 120% L/S ratio d10 curve. The relationship between drop height and steady-growth rate can be further investigated by performing single-drop granulation tests at varying heights, and

then performing the corresponding wet granulation experiments. If quantified, the relationship between drop height and growth rate is one example of how information gleaned from single-drop tests could be used to create models that would eliminate the need to run as many wet granulation trials. As the 120% L/S ratio curve shows, induction can be useful to create granules of a particle size rapidly, e.g. in 15 minutes, but is very specific in its uses and thus not a preferable growth regime to granulate in. The d10 behavior of the 130% L/S ratio visualizes how superfluous amounts of liquid decreases the strength of particles, as well as diminishes the ability to predict their growth over time. The d10 particle size could be decreasing because the larger particles are unstable and breaking due to additional shear, or the fact that the more porous particles can become compressed as the impellor continues to apply a shear to the particles throughout the wet-massing. The maximum amount of water a powder bed can take before the particles grow inductively or begin to break in size can be identified by relating hydrophobicity and particle wetting (Nguyen *et al*., 2010). Thus, a series of single-drop experiments with different hydrophobicity should be compared to a series of corresponding wet massing granulation experiments to identify additional ways to quantify the ideal L/S ratio for granule growth over time.

CHAPTER 6

INVESTIGATION OF SINGLE-DROP PARAMETERS ON HIGH-SHEAR GRANULATION

6.1 Introduction

The purpose of the final experiment was to expand upon correlations between single drop and wet granulation identified in Experiment 2, and augment the high shear granulation conditions to mimic the single drop conditions more precisely. A 0.2 mm and 2.0 mm syringe tip were added to the spray nozzle to create drops that were the same size as those used in single drop tests. The flow rate was reduced to 3 ml/min to ensure every drop was visible upon leaving the syringe, as opposed to the intermittent spray pattern that was experienced at higher spray rates. The wetting time was significantly increased by reducing the volumetric rate so dramatically, so the mass of the initial powder bed was reduced from 250 grams to 150 grams MCC. The difference in drop height was maximized for the apparatus, although the difference was only approximately 2 cm. Finally, a low and high L/S ratio of 80% and 120% were chosen from the prior two experiments to compare the effects of sufficient wetting in the powder bed. From Experiment 2, it was found that a L/S ratio of 120% would create granules at least 1mm in diameter, so the solidity, diameter, and circularity of said granules were analyzed in a Malvern Morphologi G3 to better investigate how the single-drop parameters affected the morphology of high shear granulated particles.

6.2 Results

The results show that the cumulative distribution for the 120% L/S ratio versus the 80% L/S ratio is substantially different, and thus the two have been separated for graphing purposes. Similar to Experiment 1, duplicates were taken and the standard deviation between values were used to calculate errors, but the error bars have been omitted to not clutter the graphs. Errors can be found in Appendix B-3. All of the cumulative distributions have a final value less than 100% since the granules larger than 4 mm were removed because these few granules heavily skewed the distributions due to large granules weighing up to 5 grams. Some combinations of MCC larger than 4 mm were not true granules, but rather dried up cake from the granulator as seen in Figure 11.

Figure 11. Examples of two combinations of MCC and water greater than 4 mm: dried cake from the impellor blade (left) and a large irregular granule (right).

Since particles larger than 4 mm were removed from the cumulative distribution plots, the lower hydration samples all had a final cumulative distribution significantly lower than the 120% L/S ratio equivalent trial, as seen in Figure 12 below.

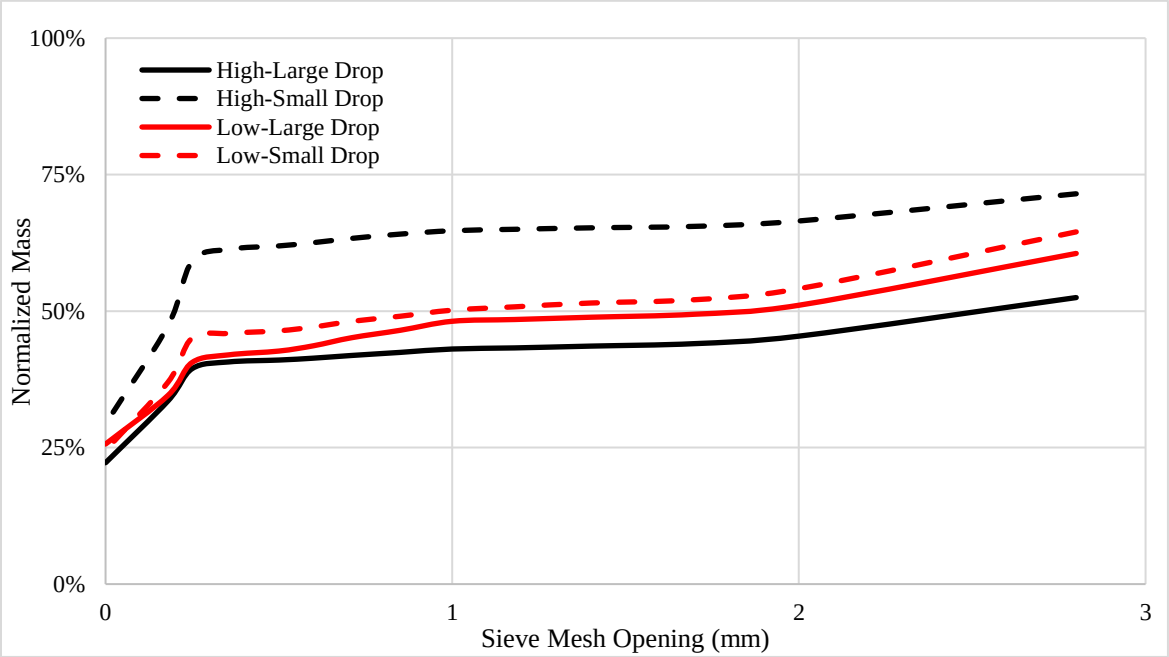

Figure 12. The normalized mass distribution versus the sieve mesh opening for the 4 80% L/S trials in Experiment 3. The red line is the low drop height, and the dashed line is the small drop size.

Three of the four trials represented above had a d25 value less or around zero. For both of the low drop height trials, about 20% of the granules existed between 0.25 and 3 mm, as opposed to both the high drop heights, which only had about 10% of the granules by mass in the same window. Of the four trials, the small drops had smaller d30 and d50 values. In contrast, at a 120% L/S ratio, the smaller drop size actually had larger d10 and d50 values by nearly 100 microns. When comparing the d50/d10 as well as the d75/d50 values, the smaller drops always had values closer to 1 than the large drop counterparts did.

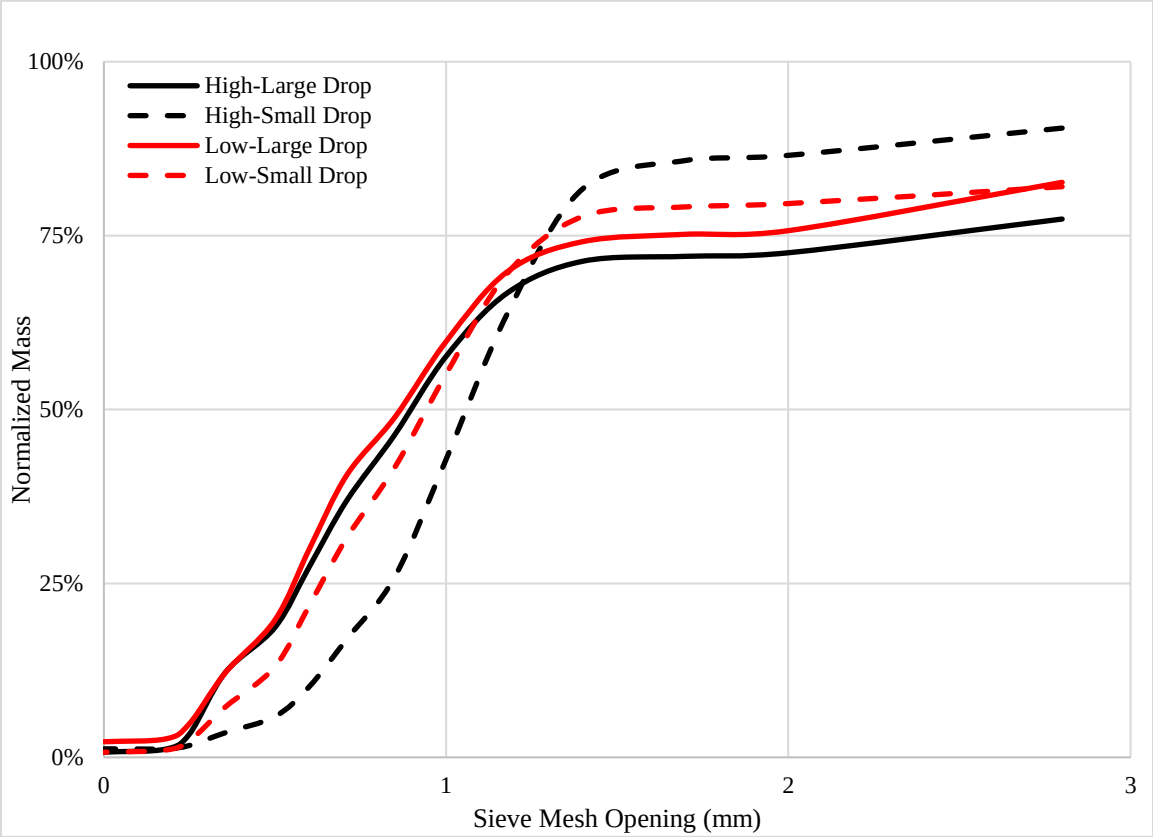

Figure 13. The normalized mass distribution versus the sieve mesh opening for the 4 120% L/S trials in Experiment 3. The red line is the low drop height, and the dashed line is the small drop size.

At the higher drop height, the small drop most closely resembles an "S" shape, while the high drop height large particle (solid black line) least resembles the "S" shape. The effect of drop size is more pronounced at a higher drop height, where the difference in final cumulative mass is 90% and 77% for small and large drops, respectively. All of the curves begin to level out around 1.5 to 2 mm.

The mean and variance for each of the average values from the 8 trials were calculated using the first and second moments, respectively, and the results were analyzed in JMP.

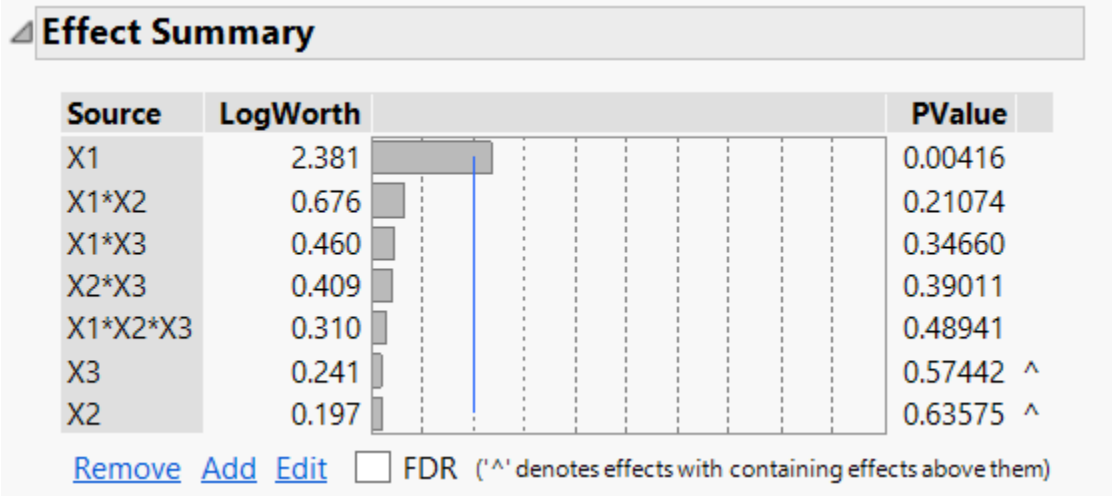

Figure 14. Pareto plot of the effects of L/S Ratio (X1), Drop Height (X2), and Drop Size (X3), on mean particle size.

The Pareto plot, Figure 14, reaffirms that L/S was the only parameter that had a statistically significant effect on the mean particle size (p-value less than 0.005). The figure above also highlights that while drop height and drop size have minimal effects as single changes in the variables, the combination of the two parameters, especially with L/S ratio, has a noticeable effect on mean particle size. Since the 120% L/S ratio created larger granules, 75 cubic millimeters of the granules that were sieved between the range of 1 mm and 1.18 mm were analyzed in the Malvern to identify the effects of drop size or height on granule shape. Circularity and solidity were calculated for 8 samples from the 8 120 % L/S trials, and the values were analyzed in JMP. A parameter profiler is seen below in Figure 15.

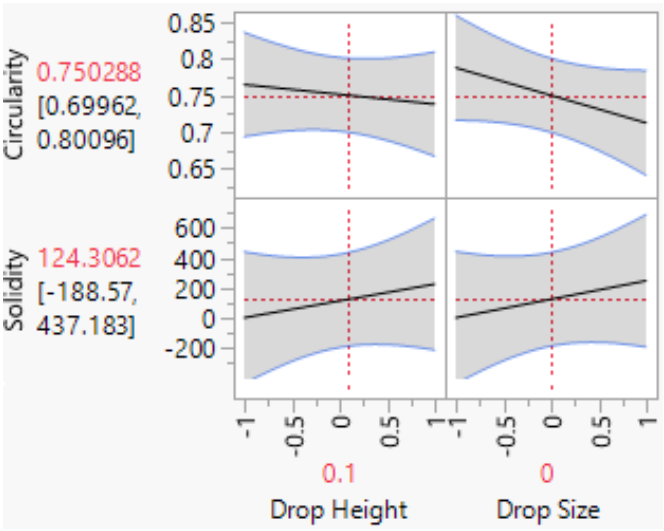

Figure 15. A parameter profiler generated in JMP for circularity and solidty of granules larger than 1 mm at low and high drop height and drop sizes.

The effects of drop height and drop size on solidity were very small. Drop height similarly had no noticeable effect on circularity. While the effect of drop size was not statistically significant, data shows that the circularity was greater for granules created from the small drops. Pictures from the Malvern are shown below to highlight the visual difference in circularity.

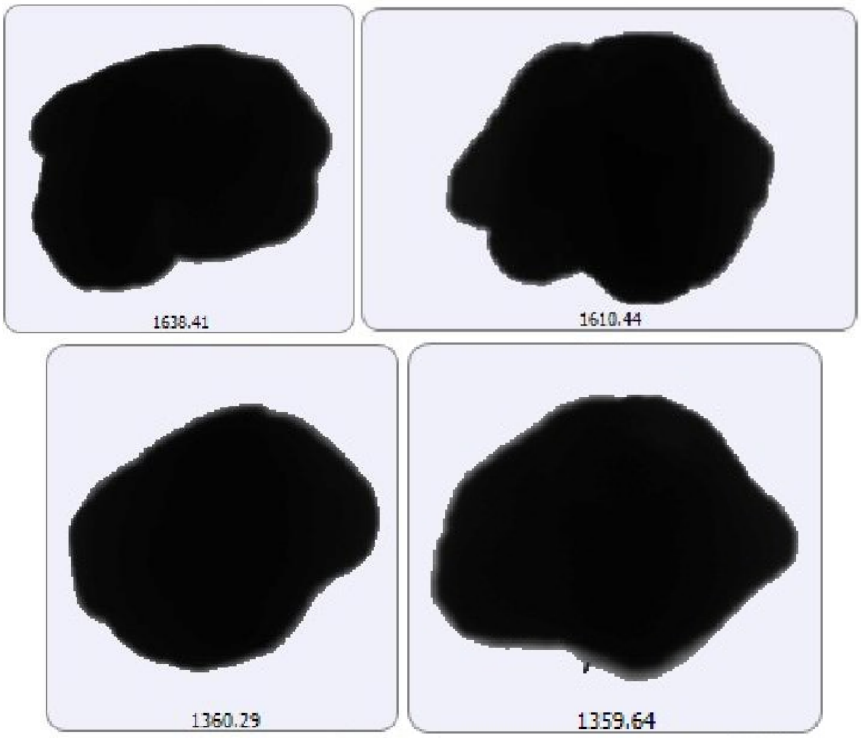

Figure 16: Images captured by the Malvern Morpholgi G3 for 120% L/S granules large than 1 mm: Top left (low/small drop) top right (low/large drop), bottom left (high/small drop), and bottom right (high/large drop).

Despite the sieves having mesh sizes of 1 mm and 1.18 mm, all four particles are at least 1.3 mm. Of the two larger particles, the smaller drop size has less significant protrusions and an overall rounder shape, seen in the top left corner of Figure 16. Similar trends are noticeable in the two smaller particles, for the higher drop height. These particles were chosen to highlight the difference in how visuals such as protrusions can be quantified by an instrument like the Malvern Morphologi G3 quantitatively by a value such as circularity. The calculations for circularity are an average value of at least 20 particles for each trial, and thus there are cases were a large droplet granule will be more circular than a small droplet granule. A more complete list of images taken from the Malvern can be seen in Appendix A-3.

6.3 Discussion

The stark contrast in the 80% and 120% L/S ratio cumulative distributions reaffirms the findings from Experiments 1 and 2, which due to the chemical properties of the MCC particles, such as its proclivity to absorb water and swell when wetted, insufficient moisture will lead to uncompleted granulation. Furthermore, at lower L/S ratios, and in the absence of a chopper, low L/S ratios of MCC and water approach nearly a bimodal size distribution, with fine powder particles and larger round granules the size of marbles, as seen in Figure 17.

Figure 17. The remaining ungranulated powder (left) and granules larger than 3 mm (right) of the 80% L/S ratio low drop height large drop size trial in Experiment 3.

Since there is insufficient water in the powder bed, even during the extended wet-massing time, large amounts of powder are hampered from undergoing initial nucleation, the precursor to granulation and particle growth. In contrast, the granules that do undergo initial wetting and nucleation continue to consolidate using the moisture of other granules to create water bridges, leading to large non-uniform granules. While 80% is obviously insufficient moisture to consistently create granules of any size, the lower drop size had

twice as many particles in the 0.250-0.3 mm range, signifying more efficient wetting of the powder bed. While increasing height decreases penetration time, and leads to more drop-controlled nucleation, the lack of hydration actually leads to the greater penetration which exacerbates the bimodal behavior. For the higher nozzle, the large drop had the lowest cumulative mass of particles less than 3 mm because a larger drop creates fewer drops per volume of water, and increased height causes greater penetration, leading to more large particles that continue to consolidate over the 60 minute wet mass time. In contrast, the small drops at a great height maximized the amount of drops that would come in and penetrate the powder bed, but lacked the initial drop size to coalesce into significant portions of granules greater than 3 mm.

Similar differences in final cumulative mass between both high drop height trials is observed for the 120% L/S ratio, signifying similar relationships between drop size and consolidation behavior, but the "S" of the curve is more pronounced. With sufficient moisture levels, the smaller drops had more narrow distributions, as shown by the tighter "S" shape, as well as the lower d10/d50 and d75/d50 values. Although a smaller drop size should increase the spray flux and create a poorer liquid distribution since the volumetric flow rate was kept constant, but the syringe aperture was decreased, the smaller drops create more sites to initiate nucleation in the bed (Hapgood *et al*., 2003). One theory for the more uniform particle size distribution, despite the poorer theoretical wetting, is that the extended wet-massing time, in combination with higher L/S ratios and induction particle growth, allows for enough mixing that discrepancies in initial nucleation are abated. While the larger drop trials were less uniform in particle size, their cumulative

distributions were practically identical, indicating more consistent particle size distributions with larger drops, albeit at the trade-off of a higher polydispersity.

Drop is a variable that can affect penetration time and spray flux respectively and drop height is a parameter that can effect initial nucleation, but as the JMP analysis shows, as individual factors they have minute effects on mean particle size, especially compared to the L/S ratio. That, however, does not mean that they are unimportant factors, nor that information from single-drop tests would not be helpful when hypothesizing particle size and polydispersity. The combination of the two effects is important because the impact of the binder with powder dictates the nucleation behavior, and the initial morphological properties of the initial granule nucleus influence how other factors, especially L/S ratio, drive the consolidation and growth of the granules. With insufficient hydration, smaller initial granules are more likely to provide the building blocks for larger granules, while at higher L/S ratios, the excess of moisture allows for more water-bridges between particles, meaning that particles not originally wetted can form granules during the wet-massing period. Therefore, the behavior of powder-binder interactions extracted from single-drop tests can be used in conjunction with knowledge of moisture effects to control mean particle size.

While the levels of parameters in Experiment 3 were not different enough to find a statistically significant effect on drop mechanisms and granule shape, initial experiments indicate an important relationship between drop size and circularity. A smaller droplet is more likely to retain its sphericity and permeate evenly as it penetrates the bed, leading to a more uniform initial nucleus whose shape will grow evenly under the constant shear of

the KG5 granulator. This behavior would have to be corroborated by future experiments comparing single-drop to wet granulation, but initial single-drop experiments have already been conducted to find the three different ways of granule formation mechanisms; the next step is then to see how those formation mechanisms contribute to wet granulation bulk properties, such as shape (Emady *et al*., 2011).

CHAPTER 7

CONCLUSION

The three experiments conducted highlight the importance of understanding the interactions between binder and powder, as well as the relationship between single drop and wet granulation. The granulation of hydrophilic MCC and water underwent steady-state growth over time at a L/S ratio of 110%, with higher moisture ratios leading to induction growth that grew more severe at increasing flow rates. Ratios below a 100% L/S ratio led to bimodal distributions of un-granulated powder and large, irregular particles, a behavior not observed in other powders, such as zirconium hydroxide(Adepu et al., 2016). The unique interactions between solids and binding agents contingent on myriad chemical properties, such as the effects of hydrophobicity, can be investigated independent of wet granulation methods, and the information found used to test the ideal L/S ratio between binders and solids conducive to steady-state granule growth. At the steady-state particle growth, increasing the drop height decreased the rate at which granules grew, demonstrating that the rate of particle growth can be augmented without compromising the growth regime. Manufacturing granules in the linear growth regime is important because it allows manufacturers more control over the exact size of their granulation by altering wet-massing time instead of worrying about fine tuning a granulator operating under induction steady-state growth. In industry, less fine tuning means less sample wasted on unsuccessful granulation and greater energy and cost savings.

The experiments demonstrated that factors easily altered in single-drop granulation experiments, such as drop height and drop size, had little individual effect on the growth

of particles, but their combined effects, such as large drops from a high height, can lead to deviations in desired granulation, such as large irregular granules. Hapgood *et al.* have created regimes that predict the nucleation behavior of particles, but there are currently no correlations that quantify how the change in parameters such as drop size affect desired particle traits such as size and shape (Hapgood *et al.*, 2003). The preliminary DOE experiments conducted demonstrated that factors such as reducing the drop size at appropriate moisture levels can actually increase the median particle size. Quantifying the effects of drop size and drop height further would allow for investigators to test the effects of drop height and size in quick single drop experiments and model the behavior of wet granulation without conducting the lengthy experiments, saving time and money. Furthermore, the ability to alter growth rate without altering L/S ratio allows for those in industry to adjust and optimize the growth rate of their system without compromising the chemical composition of their granules.

Information obtained from single drop experiments, such as granule formulation mechanisms, can also be used to hypothesize important morphological properties of granules during nucleation, as well as consolidation and growth. The preliminary experiments highlight the relationship between decreasing drop size and an increase in granule circularity, a trend that if further quantified through single-drop experiments and wet granulation validation would allow models to more accurately predict final granule shape as well as size.

Extensive research has been conducted in the field of wet granulation to estimate the empirical growth patterns of agglomerating solids undergoing constant shear. Single liquid

and particle experiments have also been performed to characterize important interactions such as penetration and wetting. However, little research has been done to correlate single-drop and wet granulation findings to create quantitative models that predict particle shape, size, and size distribution through correlating the aforementioned relationship between the phenomena that drive both types of granulation. This paper does not propose a new predictive granulation model, but rather screens for the pertinent factors ubiquitous to single drop and wet granulation and identifies initial patterns. The long term goal of this research is to create a quantitative model for high-shear granulation to be used in industry that can be optimized for a given combination of binding agent and powder by quantifying fundamental chemical interactions such as wetting effects through simple single drop granulation experiments.

Moving forward, wet granulation experiments of varying drop size for a 110% L/S ratio of water with MCC should be conducted to identify and quantify the trend between drop size and mean particle size during steady-state growth. If a relationship is identified, then single-drop experiments of the same moisture level and varying drop sizes should be performed to relate single-drop and wet granulation. Similar experiments should be performed at varying drop heights and 110% L/S ratio so that instead of having regimes that identify the type of nucleation happening during granulation, the single drop experiments can be used define a numeric relationship between drop height and mean granule size. The past two decades have shown marked progress in the identification of granulation mechanisms, but this paper highlights the need to synthesize knowledge from both single-drop and wet granulation to develop integrated, specific, and quantitative

granulation models that will lead to large cost and energy savings in an industry that already has a 1 trillion economic contribution to the United States economy (Litster, 2016)

REFERENCES

Adepu, M., Hate, S., Bétard, A., Oka, S., Schongut, M., Sen, M., … Ramachandran, R. (2016). Quantitative validation and analysis of the regime map approach for the wet granulation of industrially relevant zirconium hydroxide powders. *Powder Technology*. http://doi.org/10.1016/j.powtec.2016.02.026

Badawy, S. I. F., & Hussain, M. A. (2004). Effect of starting material particle size on its agglomeration behavior in high shear wet granulation. *AAPS PharmSciTech*. http://doi.org/10.1208/pt050338

Bouwman, A. M., Henstra, M. J., Westerman, D., Chung, J. T., Zhang, Z., Ingram, A., … Frijlink, H. W. (2005). The effect of the amount of binder liquid on the granulation mechanisms and structure of microcrystalline cellulose granules prepared by high shear granulation. *International Journal of Pharmaceutics*, *290*(1–2), 129–136. http://doi.org/10.1016/J.IJPHARM.2004.11.024

Emady, H. N., Kayrak-Talay, D., Schwerin, W. C., & Litster, J. D. (2011). Granule formation mechanisms and morphology from single drop impact on powder beds. *Powder Technology*, *212*(1), 69–79. http://doi.org/10.1016/J.POWTEC.2011.04.030

Hapgood, K. P., Litster, J. D., & Smith, R. (2003). Nucleation regime map for liquid bound granules. *AIChE Journal*. http://doi.org/10.1002/aic.690490207

Heertjes, P. M., & Kossen, N. W. F. (1967). Measuring the contact angles of powder-liquid systems. *Powder Technology*, *1*(1), 33–42. http://doi.org/10.1016/0032-5910(67)80006-8

Iveson, S. M., & Luster, J. D. (1998). Growth regime map for liquid-bound granules. *AIChE Journal*. http://doi.org/10.1002/aic.690440705

Litster, J. (2016). *Design and Processing of Particulate Products*. (A. Varma, Ed.) (1st ed.). Cambridge: Cambridge University Press.

Nguyen, T. H., Shen, W., & Hapgood, K. (2010). Effect of formulation hydrophobicity on drug distribution in wet granulation. *Chemical Engineering Journal*, *164*(2–3), 330–339. http://doi.org/10.1016/J.CEJ.2010.05.008

Pohlman, D. A., & Litster, J. D. (2015). Coalescence model for induction growth behavior in high shear granulation. *Powder Technology*, *270*, 435–444. http://doi.org/10.1016/J.POWTEC.2014.07.016

Scott, A. ., Hounslow, M. ., & Instone, T. (2000). Direct evidence of heterogeneity during high-shear granulation. *Powder Technology*, *113*(1–2), 205–213. http://doi.org/10.1016/S0032-5910(00)00354-5

Wildeboer, W. J., Koppendraaier, E., Litster, J. D., Howes, T., & Meesters, G. (2007). A novel nucleation apparatus for regime separated granulation. *Powder Technology*, *171*(2), 96–105. http://doi.org/10.1016/J.POWTEC.2006.09.008

APPENDIX A

RAW DATA COLLECTED JANUARY 2018- MARCH 2010

APPENDIX A

RAW DATA

A-1 EXPERIMENT 1

Table A-1. The raw mass distribution per sieve for each of the 16 trials in Experiment 1.

Batch #	Granulator Date	Sieve Date	Wetting Time (min)	Flow Rate (mL/min)	Total Water (mL)	Impeller Speed (rpm)	Mass Particles (g) per Sieve Mesh Size (mm)										
							1.000	.850	0.710	0.600	0.500	0.355	0.250	0.180	0.125	Bot	Total
1	1/11/18	1/13/18	10	20	200	250	12.1	5.6	5	3.3	2.2	7	44.8	49.6	49.1	35.2	213.9
2	1/13/18	1/16/18	10	20	200	325	3.1	0.3	0.3	0.6	1.6	16.3	54.8	52.4	51.4	48.4	229.2
3	1/16/18	1/17/18	10	22.5	225	250	9.1	0.6	1.1	2.7	5.7	40.2	67.9	48.8	36.4	28	240.5
4	1/16/18	1/17/18	10	22.5	225	325	4.1	1.4	6	12.9	20.6	51	71.3	66.3	29.7	2.9	266.2
5	1/17/18	1/18/18	20	10	200	250	13.5	1.2	1.4	2.2	3.6	19.3	50.5	52.2	49.8	50.4	244.1
6	1/19/18	1/20/18	20	10	200	325	0.8	0.2	0.6	1	1.5	12.5	31.7	49.2	61.3	90.7	249.5
7	1/19/18	1/20/18	20	11.3	226	250	8.9	0.6	1.3	3.6	7.5	47.9	75.7	42.7	30.6	22.6	241.4
8	1/20/18	1/21/18	20	11.2	224	325	3.1	0.4	1.3	0.9	4.7	28.5	49.5	54.5	52.5	53.3	248.7
9	1/23/18	1/24/18	20	11.3	226	325	1.8	0.6	1.5	3.3	8.4	31.0	68.2	62.7	88.7	4.0	270.2
10	1/24/18	1/27/18	20	10	200	325	0.8	0.5	2.0	3.2	1.4	25.6	55.7	43.3	50.6	54.7	237.8
11	1/27/18	1/29/18	10	20	200	250	10.6	4.3	4.9	4.8	3.5	7.7	15.9	30.0	56.4	92.4	230.5
12	1/27/18	1/29/18	10	22.5	225	325	1.9	0.4	1.9	7.5	12.3	66.5	81.9	31.3	30.5	5.9	240.1
13	1/29/18	1/31/18	20	10	200	250	4.5	1.0	1.5	2.6	2.9	9.9	57.7	44.3	48.0	60.9	233.3
14	1/31/18	2/6/18	20	11.3	226	250	5.1	0.3	0.9	3.8	6.7	63.1	79.5	33.8	21.7	15.8	230.7
15	2/6/8	2/7/18	10	22.5	225	250	5.2	0.8	2.1	4.1	8.9	53.0	79.2	48.0	41.0	21.2	263.5
16	2/7/18	2/9/18	10	20	200	325	2.6	0.1	0.6	2.5	6.4	27.4	55.9	43	49.7	48.5	236.7

A-2 EXPERIMENT 2

Table A-2.1. The raw mass distribution per sieve of the 4 L/S ratios and low drop height for Experiment 2.

Sample Time	L/S Ratio	Mass Particles (g) per Sieve Mesh Size (mm)										
		1.18	1.000	0.850	0.710	0.600	0.500	0.355	0.250	0.180	0.000	Total
0 min	100	3.1	0.5	0.3	0.2	0.2	0.3	0.6	0.8	0.6	0.7	7.3
	110	0.5	0.2	0.2	0.3	0.3	0.4	0.5	0.5	0.2	0.1	3.2
	120	3.6	0.4	0.5	0.7	0.6	0.5	0.9	0.5	0.2	0.1	8
	130	4.7	1.3	1	0.9	0.7	0.5	0.7	0.3	0.1	0	10.2
15 min	100	2.7	0.6	0.4	0.2	0.1	0.2	1.2	1.9	1	1.1	9.4
	110	5.4	1	0.9	1.2	0.8	0.8	1.1	0.7	0.1	0.1	12.1
	120	4.1	1	0.7	0.8	0.6	0.4	0.2	0.1	0.1	0	8
	130	6	0.6	0.4	0.2	0.1	0.1	0	0	0	0	7.4
30 min	100	2.5	0.1	0.1	0.1	0.3	0.6	2.5	3	1.3	1	11.5
	110	3.4	1.4	1.2	1.3	0.9	0.9	1.7	0.2	0	0	11
	120	4	1.1	0.8	0.7	0.5	0.3	0.2	0.1	0	0	7.7
	130	6.9	0.6	0.4	0.2	0.1	0	0	0	0	0	8.2
45 min	100	0.3	0.1	0	0.1	0.2	0.6	2.9	3.3	1.4	1.3	10.2
	110	2.4	1.3	1.1	1.2	1.2	1.2	0.7	0.1	0	0	9.2
	120	3.5	1.4	0.9	1	0.7	0.3	0.3	0.1	0	0	8.2
	130	5.7	0.9	0.6	0.4	0.3	0.1	0	0	0	0	8
60 min	100	2.5	0	0	0.1	0.3	0.6	3.2	3.5	1.3	1.3	12.8
	110	2.5	1.6	1.4	1.8	1.8	1.5	0.7	0.2	0	0	11.5
	120	4.4	1.6	1.1	1	0.7	0.4	0.3	0	0	0	9.5
	130	5.4	0.9	0.6	0.4	0.3	0.1	0	0	0	0	7.7

Table A-2.2. The raw mass distribution per sieve of the 4 L/S ratios and high drop height for Experiment 2.

Sample Time	L/S Ratio	Mass Particles (g) per Sieve Mesh Size (mm)										
		1.18	1.000	0.850	0.710	0.600	0.500	0.355	0.250	0.180	0.000	Total
0 min	100	3.5	0.4	0.3	0.2	0.3	0.2	0.6	1	0.8	0.9	0.9
	110	5.4	0.5	0.4	0.4	0.7	0.6	1.3	1.1	0.6	0.3	0.1
	120	4.7	0.8	1.1	1.3	1.3	1	1.6	0.9	0.3	0	0
	130	5.7	1.7	1.4	1.1	1.1	0.6	1	0.5	0.1	0	0
15 min	100	2.5	0.8	0.7	0.4	0.3	0.2	0.3	1.3	1.2	1.3	1
	110	1.4	1.1	1.2	2.2	2.1	1.5	2.2	1.7	0.5	0	0
	120	4.8	1.5	1.3	1.2	1	0.5	0.1	0.1	0	0	0
	130	8.3	1	0.7	0.5	0.3	0.2	0.2	0.1	0	0	0
30 min	100	1.6	0.7	0.7	0.5	0.3	0.1	0.4	2.6	2.2	2	1
	110	2.1	1.4	1.7	1.7	1.7	1	1.9	1.1	0.1	0	0
	120	3.7	1.3	1.1	1.1	0.8	0.3	0.3	0	0	0	0
	130	10.7	1	0.6	0.3	0.3	0.1	0.1	0	0	0	0
45 min	100	1.1	0.3	0.1	0.1	0.1	0.1	0.5	2.1	1.6	2	1.2
	110	3.1	1.5	1.7	1.6	1.5	0.9	2.4	0.2	0	0	0
	120	5.7	2.6	1.4	1.3	0.9	0.4	0.3	0.1	0	0	0
	130	10.5	1	0.6	0.4	0.2	0.1	0.1	0	0	0	0
60 min	100	3.4	0.2	0.2	0.1	0.1	0.1	0.6	2.7	2.1	2.8	0.8
	110	1.9	1.4	1.4	1.4	1.3	1.5	1.7	0.1	0	0	0
	120	5.8	1.5	1.4	1.4	1.1	0.5	0.3	0	0	0	0
	130	8.4	1.5	0.9	0.7	0.5	0.1	0.1	0	0	0	0

A-3 EXPERIMENT 3

Table A-3.1. The raw mass distribution per sieve for each of the 16 trials in Experiment 3.

Run Date	L/S Ratio	Drop Height	Drop Size	Mass Particles (g) per Sieve Mesh Size (mm)														
				2.8	2.0	1.7	1.4	1.18	1.0	.85	.71	.60	.50	.36	.25	.18	0	Total	4mm+
11/14/18	120	High	Large	2	0.7	1	6	11.6	11.9	8.6	7.9	5.7	3.1	2.4	0.7	0	0.5	78	15.9
2/18/19	120	High	Large	5.8	0.1	0.1	1.1	2.8	5.9	6.4	7.3	8.2	7.3	11.9	2.8	0.7	0.7	81.3	20.2
2/13/19	120	High	Small	3.2	0.6	3.3	14.6	17.2	13.8	7.3	5.6	3.5	1.9	1.5	0.4	0	1	81.7	7.8
3/15/19	120	High	Small	0.7	0.4	0.3	2.9	34	8.9	7.4	10	9.8	6.5	6.3	2	0.4	0.8	112.8	22.4
2/18/19	120	Low	Large	6.6	0.3	0.9	1.8	5	6	5.4	7.4	8.1	6.7	6.7	2.5	0	2	70	10.6
2/13/19	120	Low	Large	4.4	0.6	0.8	5.9	12.8	13	8.7	10.6	8.6	5.5	5	0.8	0.8	1.6	98.3	19.2
2/18/19	120	Low	Small	2.3	0.6	1.9	10.9	18.7	16	9.4	6.3	4.8	2.7	2.1	0.7	0.2	0.5	86	8.9
3/15/19	120	Low	Small	1.7	0.2	0.4	2.8	5.7	6.4	7.2	9.5	9.3	6.6	5.7	1.4	0.3	0.7	77.8	19.9
2/18/19	80	High	Large	4.5	0.9	0.3	0.2	0.1	0.2	0.1	0.1	0.1	0.1	0.5	2.7	4.3	8.5	39.1	16.5
2/13/19	80	High	Large	1.8	0.3	0.1	0.1	0.1	0.5	0.6	0.5	0.3	0.3	0.8	3.4	8	15.6	68.7	36.3
2/13/19	80	High	Small	4.3	0.7	0.2	0.2	0.1	0.3	0.3	0.2	0.1	0.3	1.8	11	11.4	11	54.3	12.4
3/15/19	80	High	Small	1.2	0.4	0.1	0.1	0.2	0.4	0.6	0.7	0.6	0.4	0.6	2	8.8	22.6	58.8	20.1
2/13/19	80	Low	Large	5.1	0.7	0.2	0.1	0.1	0.3	0.3	0.5	0.3	0.2	0.5	3.4	4.1	5	38.1	17.3
3/19/19	80	Low	Large	5.8	1.5	0.6	0.6	0.4	2.6	2	1.7	1.2	0.9	1.5	3.3	7.3	39.6	103.7	34.7
2/18/19	80	Low	Small	5.4	0.9	0.3	0.3	0.3	0.6	0.4	0.4	0.3	0.2	0.4	3.8	3.3	4.6	36.4	15.2
3/15/19	80	Low	Small	3.1	0.8	0.2	0.3	0.2	0.3	0.4	0.5	0.3	0.2	0.3	3	8.2	18.8	51.7	15.1

Table A-3.2. Malvern Morphologi G3 data for ~1mm particles for 8 120% L/S trials for Experiment 3

Drop Height	Drop Size	CE Diameter (micron)	Circularity	Solidity
High	Small	1348.49	0.748	0.957
Low	Small	1333.96	0.759	0.962
High	Large	1335.27	0.739	0.957
Low	Large	1215.18	0.733	0.94
High	Small	1309.7	0.831	0.978
Low	Small	1329.84	0.813	0.981
High	Large	730.35	0.635	898
Low	Large	1448.98	0.755	0.971

The following images were taken using the Malvern Morphologi G3. The results were then screenshotted and copied into this report.

Figure A-3.1. Morphologi pictures of large granules for Experiment 3 Trial: 1/11/2019 120 Low Large

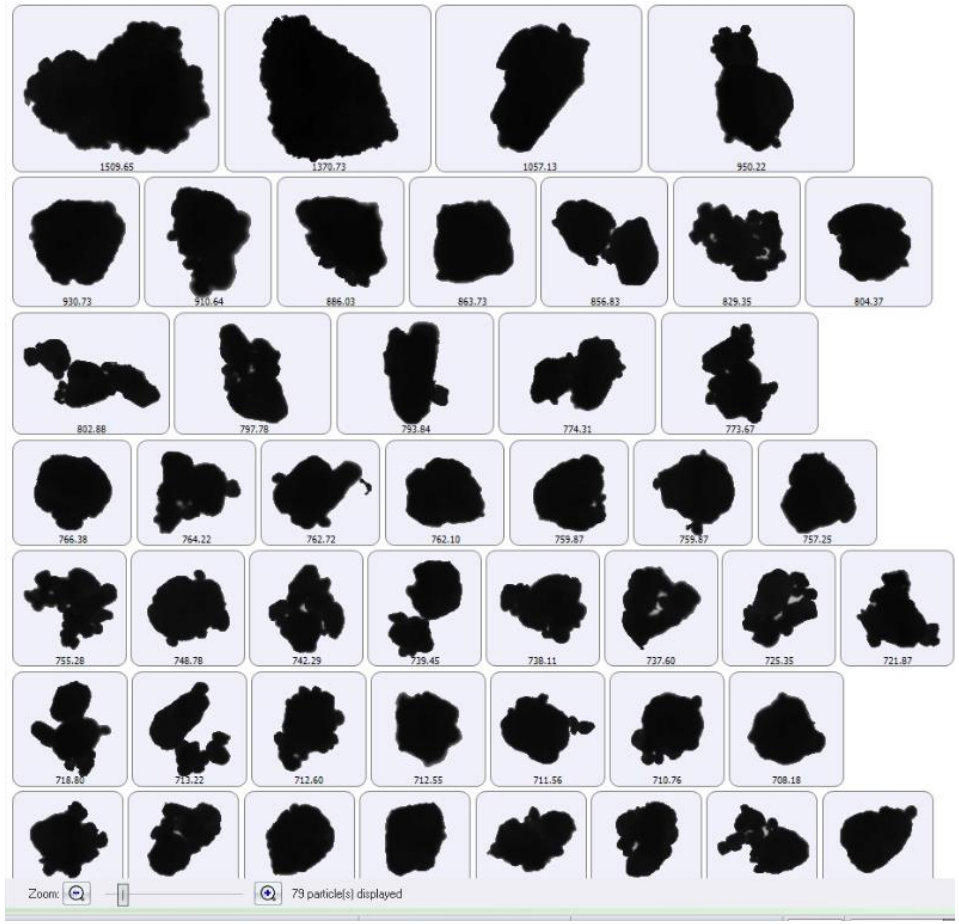

Figure A-3.2. Morphologi pictures of large granules for Experiment 3 Trial: 2/28/2019 120 High Large

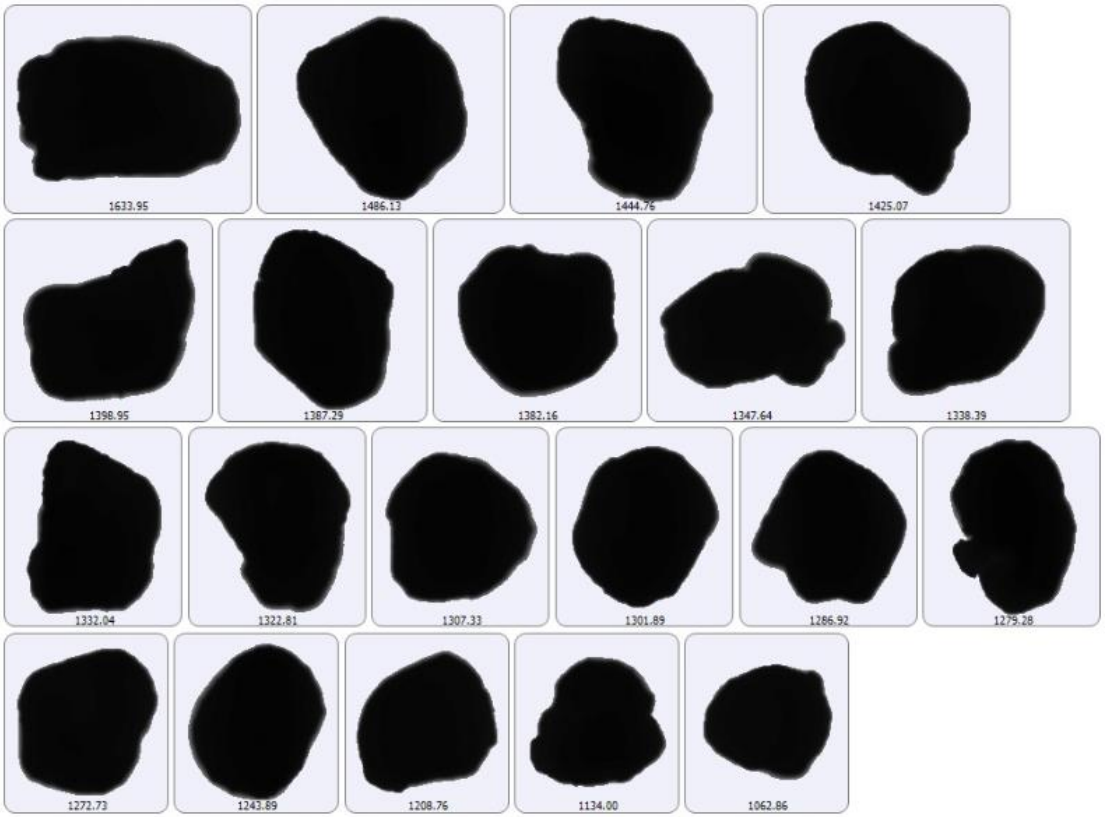

Figure A-3.3. Morphologi pictures of large granules for Experiment 3 Trial: 120 Low Small 2/19/2019

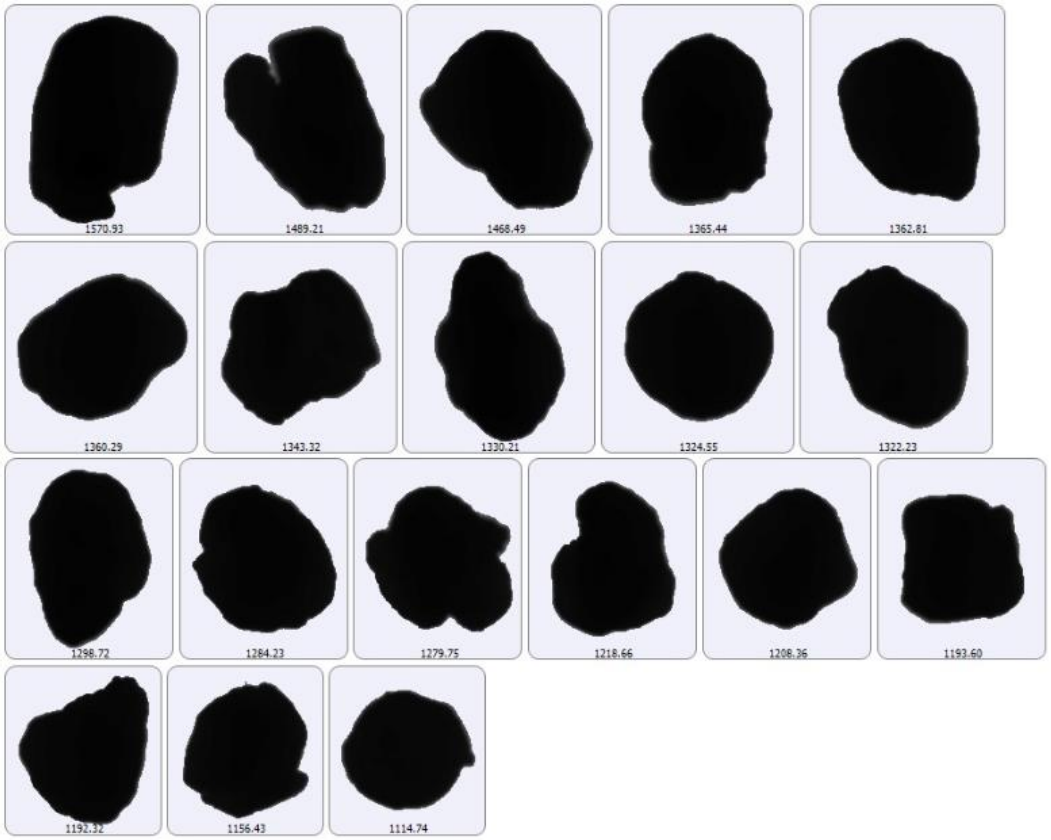

Figure A-3.4. Morphologi pictures of large granules for Experiment 3 Trial: 1/31/2019 120 High Small

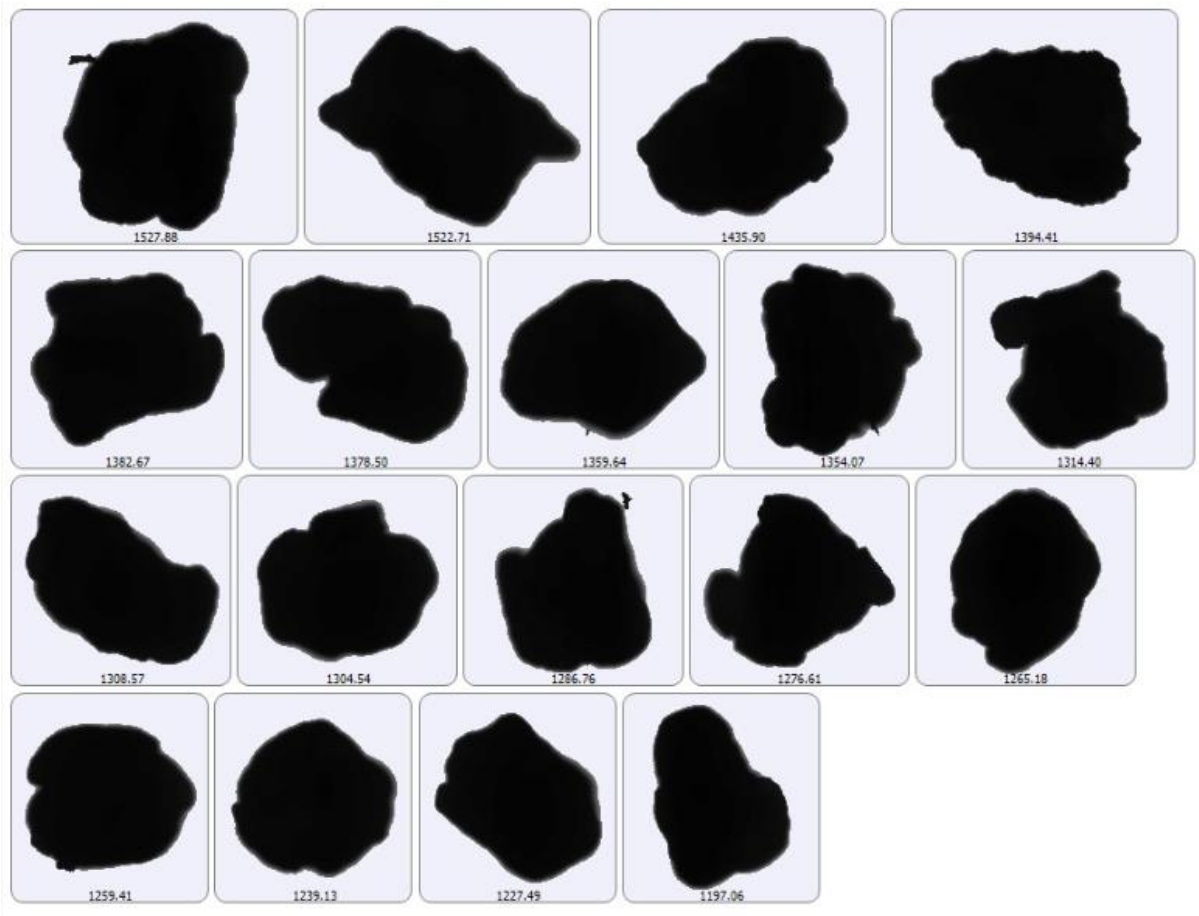

Figure A-3.5. Morphologi pictures of large granules for Experiment 3 Trial: 2/18/2019 120 High Large

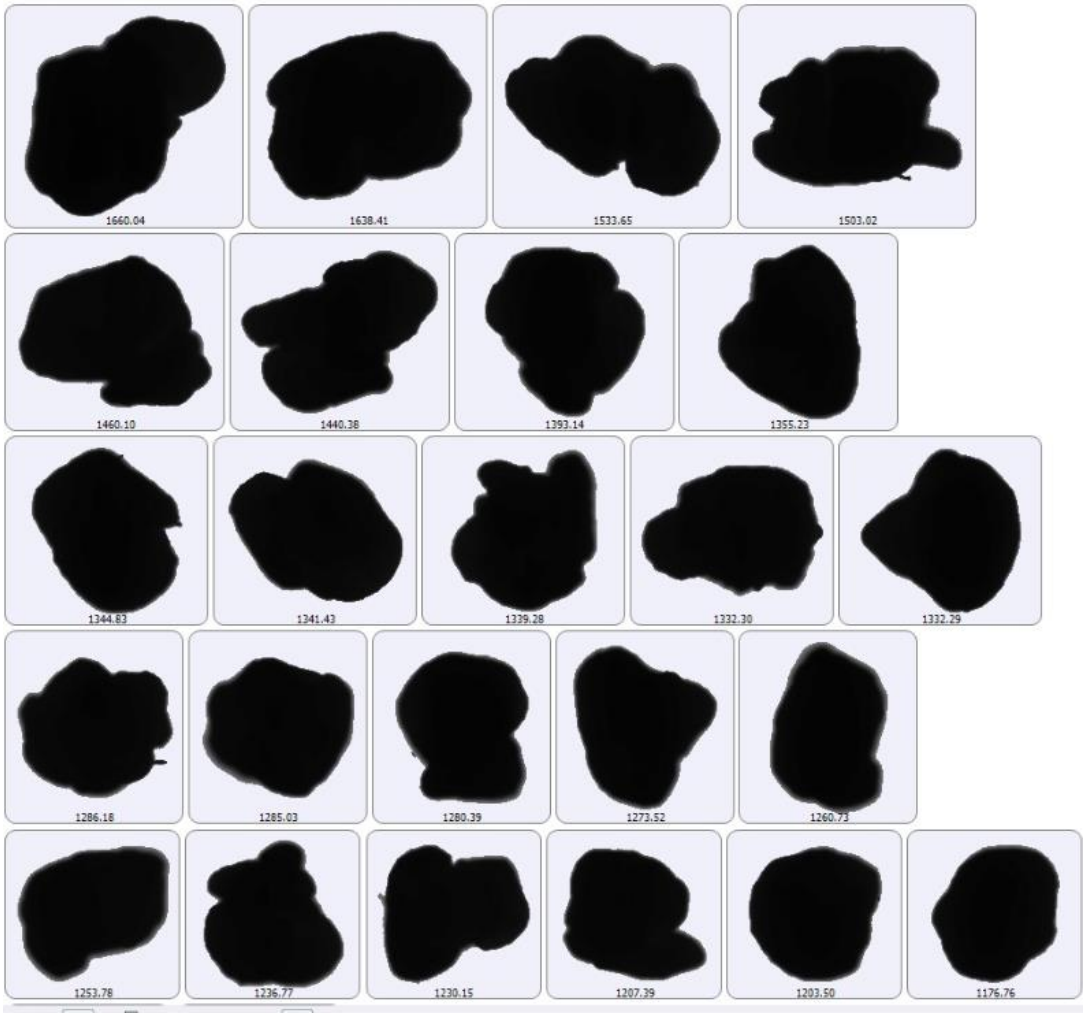

Figure A-3.6. Morphologi pictures of large granules for Experiment 3 Trial: 2/21/2109 120 Low Small

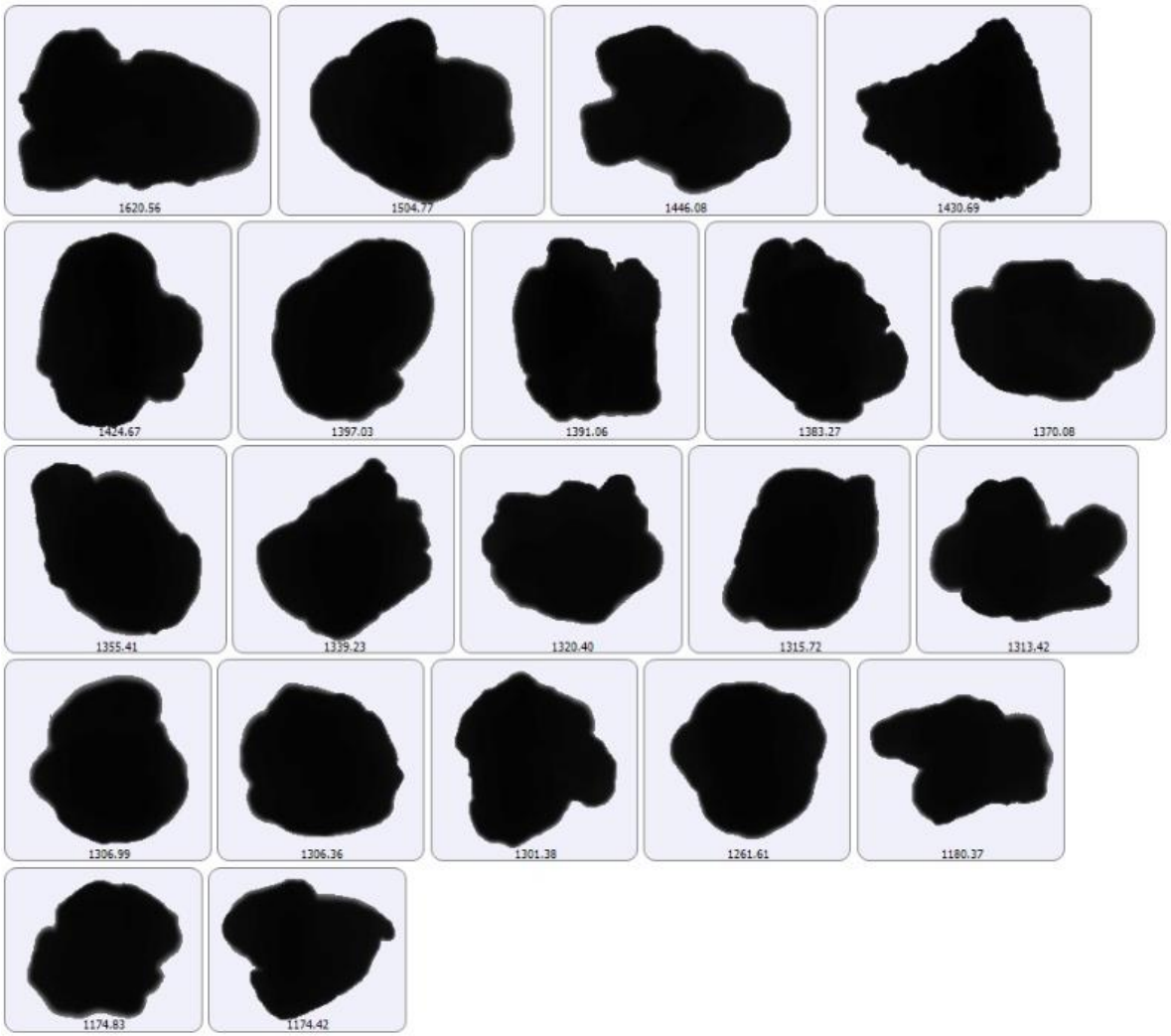

Figure A-3.7. Morphologi pictures of large granules for Experiment 3 Trial: 2/26/2019 120 High Small

APPENDIX B

CALCULATED VALUES

B-1 Experiment 1

Table B-1.1. Average values for mass distribution from Experiment 1, calculated using Excel Average function.

Batch #	Wetting Time (min)	Flow Rate (mL/min)	Total Water (mL)	Impeller Speed (rpm)	Average Mass Particles (g) per Sieve Mesh Size (mm)										
					1.000	.850	0.710	0.600	0.500	0.355	0.250	0.180	0.125	Bot	Total
1	10	20	200	250	11.4	5.0	4.9	4.0	2.8	7.3	30.4	39.8	52.8	63.8	222.2
2	10	20	200	325	2.85	0.2	0.45	1.55	4	21.85	55.35	47.7	50.55	48.45	232.95
3	10	22.5	225	250	7.1	0.7	1.6	3.4	7.3	46.6	73.6	48.4	38.7	24.6	252.0
4	10	22.5	225	325	3.0	0.9	3.9	10.2	16.5	58.8	76.6	48.8	30.1	4.4	253.2
5	20	10	200	250	9.0	1.1	1.4	2.4	3.3	14.6	54.1	48.3	48.9	55.7	238.7
6	20	10	200	325	0.8	0.4	1.3	2.1	1.4	19.1	43.7	46.3	56.0	72.7	243.7
7	20	11.3	226	250	7.0	0.5	1.1	3.7	7.1	55.5	77.6	38.3	26.2	19.2	236.1
8	20	11.3	226	325	2.5	0.5	1.4	2.1	6.5	29.8	58.9	58.6	70.6	28.7	259.5

Table B-1.2. Average error values for mass distribution from Experiment 1, calculated using Excel STDEV.P function.

Batch #	Wetting Time (min)	Flow Rate (mL/min)	Total Water (mL)	Impeller Speed (rpm)	Average Error of Mass Particles (g) per Sieve Mesh Size (mm)										
					1.000	.850	0.710	0.600	0.500	0.355	0.250	0.180	0.125	Bot	Total
1	10	20	200	250	1.1	0.9	0.1	1.1	0.9	0.5	20.4	13.9	5.2	40.4	11.7
2	10	20	200	325	0.35	0.1	0.21	1.34	3.39	7.8	0.78	6.65	1.2	0.07	5.3
3	10	22.5	225	250	2.8	0.1	0.7	1.0	2.3	9.1	8.0	0.6	3.3	4.8	16.3
4	10	22.5	225	325	1.6	0.7	2.9	3.8	5.9	11.0	7.5	24.7	0.6	2.1	18.5
5	20	10	200	250	6.4	0.1	0.1	0.3	0.5	6.6	5.1	5.6	1.3	7.4	7.6
6	20	10	200	325	0.0	0.2	1.0	1.6	0.1	9.3	17.0	4.2	7.6	25.5	8.3
7	20	11.3	226	250	2.7	0.2	0.3	0.1	0.6	10.7	2.7	6.3	6.3	4.8	7.6
8	20	11.3	226	325	0.9	0.1	0.1	1.7	2.6	1.8	13.2	5.8	25.6	34.9	15.2

B-2 Experiment 2

Table B-2.1. Cumulative values for mass distribution from Experiment 2, calculated using Excel Sum function.

Drop Height	L/S Ratio	Cumulative Normalized Mass per Sieve Mesh Size (mm)										
		1.18	1.00	.850	.710	.600	.500	.355	.250	.180	.00	Total
Low	100%	100%	74%	72%	71%	70%	69%	68%	62%	36%	18%	4%
High	100%	100%	75%	65%	53%	40%	28%	16%	2%	1%	1%	0%
Low	110%	100%	48%	36%	26%	14%	7%	3%	1%	1%	0%	0%
High	110%	100%	28%	18%	11%	6%	3%	2%	1%	0%	0%	0%
Low	120%	100%	82%	82%	81%	80%	79%	71%	46%	22%	11%	3%
High	120%	100%	72%	62%	53%	39%	19%	9%	2%	1%	0%	0%
Low	130%	100%	51%	38%	28%	16%	8%	4%	1%	0%	0%	0%
High	130%	100%	33%	22%	14%	7%	3%	2%	1%	0%	0%	0%

Table B-2.2. d10, d50, d90 values for Experiment 2 trials from plotting cumulative normalized mass versus particle size in Excel.

Batch #	d10	d50	d90	d50/d10	d90/d50	d90/d10
100-H	0.060	0.213	1.117	3.6	5.2	18.6
100-L	0.120	0.265	1.088	2.2	4.1	9.1
110-H	0.311	0.684	1.112	2.2	1.6	3.6
110-L	0.376	0.678	1.119	1.8	1.7	3.0
120-H	0.551	1.009	1.147	1.8	1.1	2.1
120-L	0.535	0.993	1.144	1.9	1.2	2.1
130-H	0.688	1.064	1.156	1.5	1.1	1.7
130-L	0.652	1.054	1.154	1.6	1.1	1.8

APPENDIX B-3

Experiment 3

Table B-3.1. Average values and average errors for mass distribution from Experiment 3, calculated using Excel Average and Sum functions, respectively.

				Mass Particles (g) per Sieve Mesh Size (mm)													
Value	L/S Ratio	Drop Height	Drop Size	2.8	2.0	1.7	1.4	1.18	1.0	.85	.71	.60	.50	.36	.25	.18	0
Average	120	High	Large	3.9	0.4	0.6	3.6	7.2	8.9	7.5	7.6	7.0	5.2	7.2	1.8	0.4	0.6
Error	120	High	Large	1.9	0.3	0.5	2.5	4.4	3.0	1.1	0.3	1.3	2.1	4.8	1.1	0.4	0.1
Average	120	High	Small	3.2	0.6	3.3	14.6	17.2	13.8	7.3	5.6	3.5	1.9	1.5	0.4	0.0	1.0
Error	120	High	Small	1.3	0.1	1.5	5.9	8.4	2.5	0.1	2.2	3.2	2.3	2.4	0.8	0.2	0.1
Average	120	Low	Large	5.5	0.5	0.9	3.9	8.9	9.5	7.1	9.0	8.4	6.1	5.9	1.7	0.4	1.8
Error	120	Low	Large	1.1	0.2	0.1	2.1	3.9	3.5	1.7	1.6	0.3	0.6	0.9	0.9	0.4	0.2
Average	120	Low	Small	2.0	0.4	1.2	6.9	12.2	11.2	8.3	7.9	7.1	4.7	3.9	1.1	0.3	0.6
Error	120	Low	Small	0.3	0.2	0.8	4.1	6.5	4.8	1.1	1.6	2.3	2.0	1.8	0.4	0.1	0.1
Average	80	High	Large	3.2	0.6	0.2	0.2	0.1	0.4	0.4	0.3	0.2	0.2	0.7	3.1	6.2	12.1
Error	80	High	Large	1.4	0.3	0.1	0.1	0.0	0.2	0.3	0.2	0.1	0.1	0.2	0.4	1.9	3.6
Average	80	High	Small	2.8	0.6	0.2	0.2	0.2	0.4	0.5	0.5	0.4	0.4	1.2	6.5	10.1	16.8
Error	80	High	Small	1.6	0.2	0.1	0.1	0.1	0.1	0.2	0.3	0.3	0.1	0.6	4.5	1.3	5.8
Average	80	Low	Large	5.5	1.1	0.4	0.4	0.3	1.5	1.2	1.1	0.8	0.6	1.0	3.4	5.7	22.3
Error	80	Low	Large	0.4	0.4	0.2	0.3	0.2	1.2	0.9	0.6	0.5	0.4	0.5	0.1	1.6	17.3
Average	80	Low	Small	4.3	0.9	0.3	0.3	0.3	0.5	0.4	0.5	0.3	0.2	0.4	3.4	5.8	11.7
Error	80	Low	Small	1.2	0.1	0.1	0.0	0.1	0.2	0.0	0.1	0.0	0.0	0.1	0.4	2.5	7.1

Table B-3.2. d10 and d50 values for Experiment 3 trials from plotting cumulative normalized mass versus particle size in Excel.

Drop Height	Drop Size	d10	d50	d75	d50/10	d75/d50
High	Large	0.325	0.896	2.42	2.76	2.70
High	Small	0.597	1.059	1.295	1.77	1.22
Low	Large	0.322	0.866	1.588	2.69	1.83
Low	Small	0.43	0.943	1.295	2.19	1.37